



Optimization and Effect of Reinforcements on the Sliding Wear Behavior of Self-Lubricating AZ91D-SiC-Gr Hybrid Composites

Sandeep Kumar Khatkar¹ · Rajeev Verma² · Sumankant³ · Sandeep Singh Kharb⁴ · Archana Thakur¹ · Raj Sharma³

Received: 17 January 2020 / Accepted: 13 May 2020 / Published online: 11 June 2020
© Springer Nature B.V. 2020

Abstract

This article statistically investigates the effect of various parameters such as material factors: silicon carbide (SiC) fraction, graphite (Gr) fraction and mechanical factors: normal load, sliding distance and speed on the sliding wear rate of self-lubricating AZ91D-SiC-Gr hybrid magnesium composites. The self-lubricating hybrid composites were fabricated using advanced vacuum assisted stir casting process. The sliding wear tests have been performed under dry conditions on pin-on-disc tribometer at 10–50 N loads, 1–3 m/s sliding speed and 1000–2000 m sliding distance. It has been examined that hybrid composites yielded improved wear resistance with reinforcement of SiC and solid lubricant graphite. ANOVA and signal-to-noise ratio investigation indicated that applied load was the most critical factor influencing the wear rate of fabricated hybrid composites followed by sliding distance. Further, the AZ91D/5SiC/5Gr hybrid composite has exhibited the best wear properties. From the SEM and EDS analysis of worn surfaces, delamination was confirmed as the dominant wear mechanism for AZ91D-SiC-Gr hybrid composites.

Keywords Hybrid magnesium composites · Sliding wear · Vacuum assisted stir casting · Solid lubricant graphite · Taguchi experimental design

1 Introduction

Being one of the major sources of energy consumption and environmental pollution, the transport industries are focusing on lightweight materials that are stronger and cheaper. The lightweight materials can reduce the weight of automobile, improves the fuel efficiency and reduce the harmful gas emission [1, 2]. Magnesium and its alloys possessing high stiffness and specific strength hence become favorable choice to meet such demands in automobile, aerospace, medical, electronic, defense and sports industries [3, 4]. The AZ91D alloy with high specific strength and good corrosion is one of the widely

used magnesium alloy in aerospace and automobile industries [5]. The applications of AZ91D alloy can be further increased in other automobile and space satellite components by improving its mechanical and wear properties simultaneously [6, 7]. Therefore in present investigation the AZ91D matrix is incorporated with SiC to enhancement its mechanical properties while solid lubricant graphite particles are added to improve wear behavior. Over the past years, many researchers have improved the mechanical properties of AZ91D by reinforcing the hard ceramics particles such as SiC, Al₂O₃, Y₂O₃, B₄C and TiC at micro and nano level [8]. The SiC was the most used reinforcement due to its good wettability in magnesium. The good wettability of SiC in magnesium is due to low surface tension of magnesium (0.599 N/mm) [9]. For AZ91D alloy presence of aluminum has tremendous influence in increasing the wettability of SiC [10]. Moreover; for better tribological properties, graphite has been widely reinforced as solid lubricant into various metal matrix like aluminum [11, 12], copper [13], nickel [14] zinc [15], magnesium [16], silver [17], and bronze [18]. The graphite having hexagonal lattice crystal structure has been used due to its low cost and easily availability. The graphite reinforced self-lubricating composites find applications in harsh or vacuum environmental conditions where lubrication using liquid lubricant is difficult or

✉ Sandeep Kumar Khatkar
sandeep.4388@cgc.edu.in

¹ Department of Mechanical Engineering, Chandigarh Engineering College, Landran, Punjab, India

² Industrial & Production Engineering, Dr B R Ambedkar National Institute of Technology, Jalandhar, India

³ Production & Industrial Engineering Department, Punjab Engineering College, Chandigarh, India

⁴ Poornima Institute of Engineering and Technology, Jaipur, India

impossible [19–21]. Moreover; liquid lubricants emit harmful pollutants to environment. The combination of SiC and graphite particles as a hybrid reinforcement has been extensively used by several researchers for improving the mechanical and tribological properties of different matrix such as aluminum [22–25], Copper [26, 27], and iron [15]. In this regard, Mahdavi and Akhlaghi [28] claimed that Al6061/SiC/Gr hybrid composite fabricated using in-situ powder metallurgy showed better dry sliding wear properties than base alloy and graphite reinforced composites. Krishna and Xavier [29] also found that the higher tensile strength when reinforcement of SiC and graphite as compared to Al6061 matrix alloy. Kaushik and Rao [30] reported that the Al6082/SiC/Gr hybrid composites reduces the wear compared to Al6082/SiC composites because of self-lubricating property of graphite. Maamari et al. [31] reported that reinforcement of 5 wt.% graphite particles in pure magnesium enhanced its wear resistance while slightly reducing the mechanical properties. Wang et al. [32] concluded that after forging and extrusion of AZ91/Gr composites the mechanical and wear properties were enhanced. Wu et al. [33] revealed that reinforcement of graphite particles resulted in increased tensile strength and damping capacity of AZ91 magnesium alloy. Ravindran et al. [12] found that Al2024-SiC-Gr composites exhibited superior wear resistance and lower coefficient of friction even at high sliding speeds due to formation of lubricating graphite layer. Zhu et al. [34] claimed that the wear properties of magnesium improved by reinforcing SiC and WoS_2 using powder metallurgy. Gowrishankar et al. [35] found that addition of graphite and TiC particles increased the mechanical and wear properties of Al6061 alloy. Stojanovic et al. [36] reported that addition of graphite to A356/SiC improves its wear behavior.

The different fabrication techniques such as powder metallurgy, disintegrated melt deposition metal (DMD) technique, stir casting, and squeeze casting have been adopted for uniform distribution of SiC and Gr particles in AZ91D alloy. In present research investigation, advanced vacuum assisted stir casting processing has been considered for fabrication of magnesium composite due to its lower fabrication cost, simplicity, ability to cast complex shapes and less destruction to reinforcement particles.

From the literature it was observed that a considerable amount of ambiguity still exist about the dry sliding wear behavior of AZ91D alloy reinforced with SiC and Gr. Furthermore, very less research has been reported to identify the effect of various parameters such as material factors: SiC

reinforcement, Gr reinforcement and mechanical factors: normal load, sliding distance and speed on the sliding wear behavior of AZ91D. In present research, an attempts has been made to find optimal value of control parameter such as SiC content, Gr content, sliding distance, normal load and sliding speed on the wear rate of AZ91D-SiC-Gr hybrid composite using Taguchi robust design methodology. The significant control parameters, their optimal combination and their percentage contributions for the wear rate of fabricated hybrid composite were also investigated by performing statistical analysis of variance (ANOVA).

2 Experimental and Statistical Procedure

2.1 Materials

The high purity AZ91D magnesium alloy supplied from Exclusive Magnesium private limited Hyderabad, India was chosen as base metal matrix. The chemical composition of AZ91D base alloy from XRF analysis is illustrated in Table 1. The SiC and graphite particles supplied by Sigma-Aldrich, US were selected as primary and secondary reinforcements respectively. The details of materials and their density and grain size are illustrated in Table 2. Moreover, Fig. 1 shows the field emission scanning electron microscope (FESEM, Hitachi, SU8010) images of both reinforcements (i.e. SiC and graphite). It has been observed that SiC has present in different sizes with sharp edges, while graphite showed flakes like structures. The microstructural examination of as cast alloy and AZ91-SiC-Gr hybrid composites were performed using inverted metallurgical microscope (Carl Zeiss). In this investigation, SiC was varied from 3 wt% to 5 wt%, while graphite content was varied at 0, 3 and 5 wt% for the fabrication of AZ91D-SiC-Gr hybrid magnesium composites using vacuum assisted bottom pouring stir casting. The schematic diagram of sample preparation is depicted in Fig. 2.

2.2 Fabrication of Hybrid Composites

AZ91D-SiC-Gr hybrid composites were prepared using bottom pouring vacuum stir casting machine (operating Voltage: 440 V, 3-Phase, 50 c/s) with K type thermocouple having melting capacity of 2 Kg (Swam-Equip Chennai, Tamil Nadu, India). The reason behind selection of vacuum stir casting was to achieve homogenous distribution of reinforcement

Table 1 Elements present and their percentage in AZ91D magnesium alloy (Wt.%)

Element	Al	Mn	Zn	Si	Cu,max	Fe, max	Mg
ASTM: B94–18	8.3–9.7	0.15–0.50	0.35–1	0.10	0.030	0.005	Rem.
From XRF	8.40	0.03	0.775	0.034	0.009	0.002	Rem.

Table 2 Details of reinforcement materials

Material details	Purity (%)	Average grain size(μm)	Density(g/cc)
Silicon carbide	99.9	37	3.21
Graphite	99.9	7	2.1

particle into AZ91D matrix with minimum porosity, which are essential factors for desirable properties of any particulate reinforced MMCs. Besides, the stir casting is one of the oldest, simple, economical technique having low fabrication cost and high production rate, used for producing complex shapes [9].

In the experimental investigation for the fabrication of magnesium hybrid composites, the 680 g ingot of AZ91D alloy was melted at 680 °C in the mild steel crucible furnace under the protection of SF6 and ultra-pure argon atmosphere. The mixing chamber supplied a mixture of SF6 and argon in the ratio of 1:3 to the furnace to provide favorable inert environment. The SiC and graphite reinforcement particles were preheated at 350 °C and 200 °C. While stirring with two blade stainless steel stirrer at 500 rpm, preheated SiC and graphite were added. The stirring time was varied according to the content of reinforcement for the uniform distribution of reinforcements, e.g. for a total (SiC+Gr) 10 wt% reinforcement the stirring time was 15 min. The molten melt was poured at 700 °C into the preheated mild steel mould with vacuum pouring facility. Vacuum of 10–1 mbar has been created around pouring hole using rotary vacuum pump. The mould has two cylindrical cavities of 25 mm and 23 mm diameter, 30 mm length each and one cubical cavity of 10 mm side. The sample for wear and hardness tests were prepared by machining solidified castings of hybrid composites using a carbide tip inserted single point cutting tool (SPCT) on lathe machine. Carbide tip inserted SPCT was recommended because wear rate of mild steel SPCT during machining of hybrid composites was very high due to presence of SiC, which resulted in tool damage and further reduced the surface finish.

2.3 Density and Hardness Measurement

The density of AZ91D alloy, AZ91D-SiC and AZ91D-SiC-Gr hybrid composites were measured using a density measurement kit as per ASTM standard: B962–08. Specimens were sequentially polished using emery papers of grades 800, 1000, 1500 and 2000. The weight of samples in air (W_{air}) and weight of samples suspended in distilled water (W_{water}) was measured using a electronics weighing balance with an accuracy of 0.0001 g. The actual densities of samples (ρ_a) were calculated using following Eq. (1). Ten measurements were taken for each specimen and mean value was considered as actual density of sample. The micro-hardness and density of the different fabricated hybrid magnesium composites are further illustrated in results section.

$$\rho_a = \frac{W_{\text{air}}}{(W_{\text{air}} - W_{\text{water}}) \rho_{\text{water}}} \quad (1)$$

Micro hardness of the fabricated magnesium hybrid composites was evaluated using Vickers's micro-hardness tester at room temperature. A square based pyramid diamond with a face angle 136° type indenter was used to mark an indent on specimens. A load of 100gf was applied for 10 s (dwell time) as per the ASTM: E384–99. For each specimen, five repetitions at least 5-times the diagonal distance apart were conducted to obtain normalized values.

2.4 Wear Test

The sliding wear tests were performed on the pin-on-disc tribometer (Cenlub Industries Ltd. India) under dry condition and approximately 35 °C ambient temperature. The wear test specimens of 40 mm height and 8 mm dia. Were prepared in accordance with ASTM standard G99–17. The cylindrical specimens were placed in perpendicular direction against the EN31 steel disk (63HRC) for the sliding action. The sliding

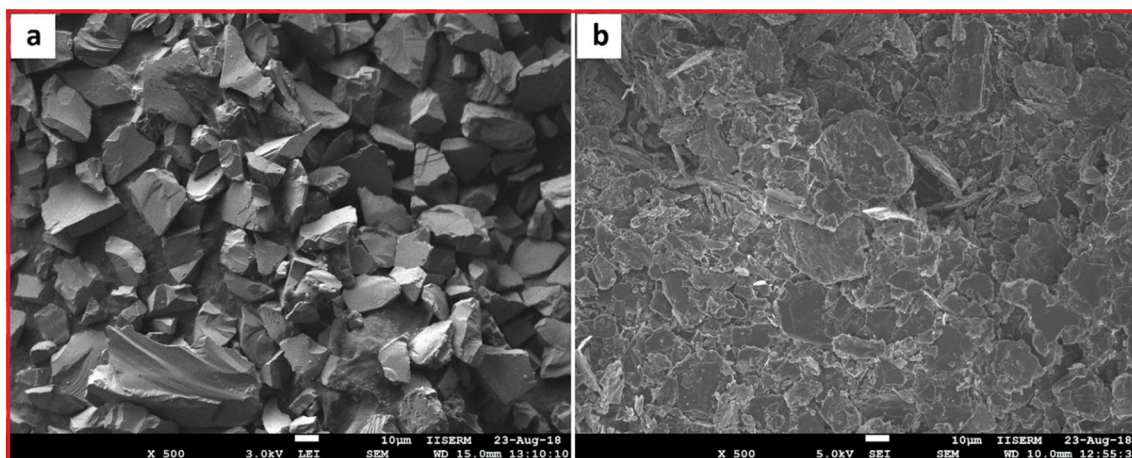
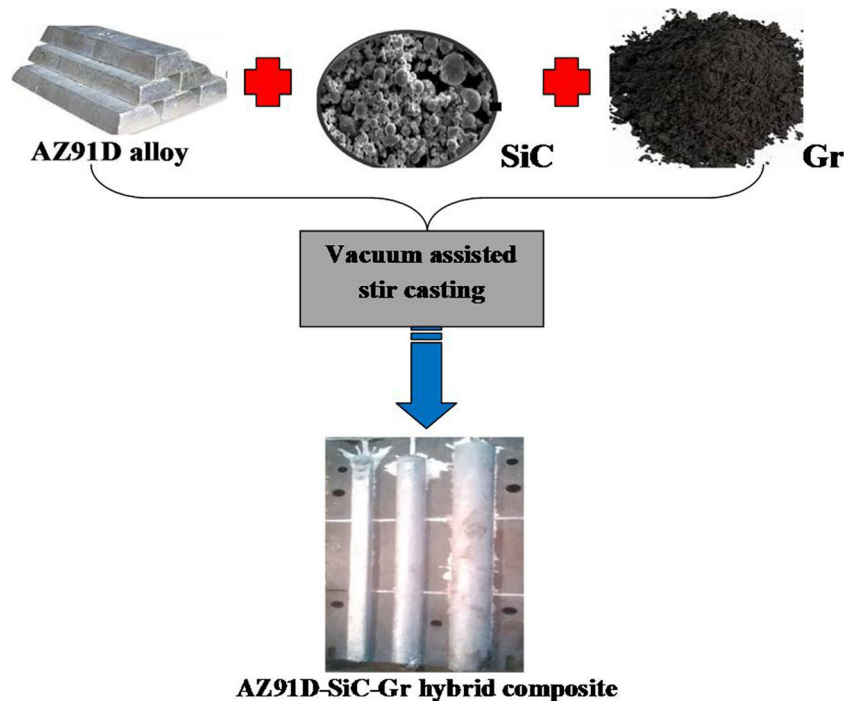


Fig. 1 FESEM analysis of reinforcement's particles at 500X magnification **a** SiC and **b** graphite

Fig. 2 Schematic diagram for casting sample preparation



wear test was performed at different loads 10,30,50 N, sliding speed 1,2,3 m/s and sliding distances 500,1000,1500 m while maintaining a track radius of 45 mm from the center of disk.

While calculating the volumetric wear rate by weight loss method, the weight of specimens before and after the wear test was measured using four digit weighing balance with an accuracy of 0.0001 g. The steel counter disk was cleaned after each wear test with acetone to remove the unwanted debris, traces of grease or other contaminants. Wear rate calculations were made according to relation in Eqs. (2) and (3) [28, 37].

$$\text{Volumetric wear rate} \left(\frac{\text{mm}^3}{\text{m}} \right) = \frac{\text{Volume loss in mm}^3}{\text{Sliding distance in m}} \quad (2)$$

$$\text{Volume loss in (mm}^3 \text{)} = \frac{\text{Weight loss in g}}{\text{density in g/mm}^3} \quad (3)$$

*Sliding distance (m) = 2πr * rpm * time(min.), where distance from the center of the disk (r) = 45 mm for each test.*

2.5 Taguchi Experimental Design

Taguchi statistical approach has been implemented for the design of experiments (DOE). Taguchi gives a standard array to calculate effect of various control factors on the response function and defines the experimental plan [38]. The variable control factors and their levels are described in Table 3. In this statistical investigation, L_{18} orthogonal array has used as shown in Table 4. Five factors have been selected for this experimentation, keeping one factor (A) at two levels and other four factors at three levels. The content of SiC, content

of graphite, applied load, sliding distance, sliding speed have been chosen as controllable factors. The notion behind considering these controllable factors for this study is to make developed hybrid magnesium composite robust.

In present statistical examination, output experimental results of wear rate were further transformed in S/N ratios using “smaller is the better” quality characteristics which are expressed as a logarithmic transformation of loss function [39], given by Eq. (4).

$$S/N = -10 \log \frac{1}{n} (\sum y_i^2) \quad (4)$$

Where ‘n’ represents the repetition of each trail/observations and y is the wear rate of the *i*-th experiment for each trail (observed data). The smaller the better quality characteristics were selected as goal of experimentation model was to minimize the response i.e. volumetric wear rate.

Table 3 The various control factors and their range of investigation

Control factors	Units	Level I	Level II	Level III
SiC percentage (A)	wt.%	3	5	*
Graphite percentage (G)	wt.%	0	3	5
Applied Load (L)	N	10	30	50
Sliding speed (S)	m/s	1	2	3
Sliding distance (D)	m	500	1000	1500

Table 4 Design of experimental using Taguchi's L_{18} orthogonal array

S. No.	A	G	A*G	L	A*L	G*L	S	D	Wear rate (mm ³ /m)	S/N ratio
1.	3	0	1	10	1	1	1	1000	0.0107	39.4123
2.	3	0	2	30	2	2	2	1500	0.0199	34.0229
3.	3	0	3	50	3	3	3	2000	0.0225	32.9563
4.	3	3	1	10	2	2	3	2000	0.0191	34.3793
5.	3	3	2	30	3	3	1	1000	0.0117	38.6363
6.	3	3	3	50	1	1	2	1500	0.0155	36.1934
7.	3	5	1	30	1	3	2	2000	0.0168	35.4938
8.	3	5	2	50	2	1	3	1000	0.0184	34.7036
9.	3	5	3	10	3	2	1	1500	0.0079	42.0475
10.	5	0	1	50	3	2	2	1000	0.0142	36.9542
11.	5	0	2	10	1	3	3	1500	0.0135	37.3933
12.	5	0	3	30	2	1	1	2000	0.0168	35.4938
13.	5	3	1	30	3	1	3	1500	0.0154	36.2496
14.	5	3	2	50	1	2	1	2000	0.0186	34.6097
15.	5	3	3	10	2	3	2	1000	0.0054	45.3521
16.	5	5	1	50	2	3	1	1500	0.0142	36.9542
17.	5	5	2	10	3	1	2	2000	0.0125	38.0618
18.	5	5	3	30	1	2	3	1000	0.0116	38.7108

mean wear rate (T_w) = 0.0147; mean S/N ratio ($T_{S/N}$) = 37.09

3 Results and Discussion

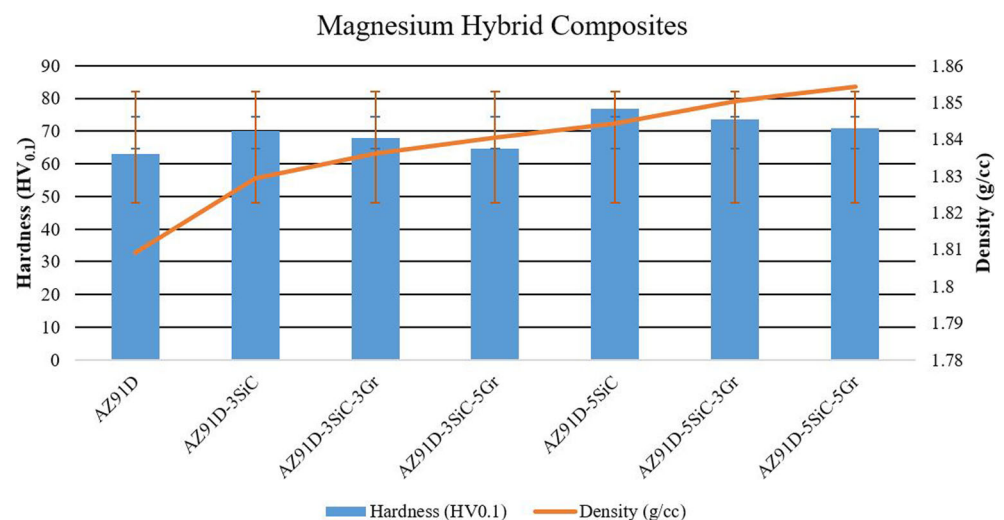
3.1 Physical and Mechanical Properties

Hardness and density of the magnesium hybrid composites were illustrated in Fig. 3. The highest value (76.9 HV) of micro-hardness was observed for AZ91D-5SiC composite, while AZ91D-3SiC-5Gr hybrid composite (64.6 HV) exhibited lowest hardness. It was clearly observed that the micro hardness of AZ91D-SiC-Gr hybrid magnesium composites were increase with increase in SiC content, while it decreases with increase in graphite content. There was an improvement of 21.87% in micro hardness of the AZ91D base matrix when

it was reinforced with 5 wt.% SiC. The presence of hard SiC particle shares most of the external applied load and also hinders the plastic deformation of AZ91D matrix and results in higher hardness.

It has also been earlier confirmed by Prakash et al. [40] that with addition of 10 wt% SiC in pure magnesium micro hardness of Mg increased from 30 HV to 80 HV, however, 10 wt% graphite addition in Mg matrix, reduced the hardness value from 30 to 24 HV. Moreover, Aathisugan et al. [10] also found out that reinforcement of 1.5 wt% B_4C in the AZ91D magnesium alloy increased the hardness from 20.1 to 27.1BHN while with addition of graphite of 1.5 wt% in AZ91D- B_4C composite decreased the hardness to 22.5BHN.

Fig. 3 Density and micro hardness of fabricated magnesium hybrid composites



It was examined that hybrid magnesium composites possessed higher density values than that of AZ91D matrix alloy. This was attributed due to reinforcement of higher density SiC and graphite. Microstructure of AZ91D-5SiC composite, AZ91D + 3SiC + 3Gr, AZ91D + 5SiC + 3Gr, and AZ91D + 5SiC + 5Gr hybrid composites has been illustrated in Fig. 4a–d respectively. The microstructural study of hybrid magnesium composites exhibited the uniformly distribution of SiC and graphite particles in the AZ91D base alloy. No slag and oxides inclusion were observed in the cast magnesium composites and hybrid composites. This homogenous distribution of reinforcements was due to the stirring action of two-blade stainless steel stirrer and vacuum pouring of molten melt. Aravindan et al. [41], and Poddar et al. [9] demonstrated that the homogenous distribution of SiC particles in AZ91 matrix can be achieved while using stir casting fabrication technique.

3.2 Statistical Analysis on Volumetric Wear Rate

The effect of various input parameters such as a) material parameters, SiC%, Gr%, b) mechanical parameters, sliding distance, sliding speed and normal loads has been assessed with S/N ratio response analysis. The weight loss and transformed S/N ratio of all hybrid magnesium composites for all experimental trails has been demonstrated in Table 5.

From the response Table 5 for data means, it was found that effect of control factors on the volumetric wear rate was in following order i.e. applied load >sliding distance>sliding speed> Gr content>SiC content.

Table 5 Response table for means for “Smaller is better”

Level	A	G	L	S	D
1	0.01583	0.01627	0.01152	0.01332	0.01200
2	0.01358	0.01428	0.01537	0.01405	0.01440
3		0.01357	0.01723	0.01675	0.01772
Delta	0.00226	0.00270	0.00572	0.00343	0.00572
Rank	5	4	1	3	2

Figure 5 shows the main effect plots for means of various input parameters with wear rate of AZ91D-SiC-Gr hybrid composites while Fig. 6 illustrated the intersection plot for wear rate. From the S/N ratios analysis, it was investigated that the optimal parameter combination for minimal volumetric wear rate was 5% SiC (A_2), 5% Gr (G_3), 10 N Load (L_1), 1 m/s sliding speed (S_1) and 1000 m lowest sliding distance (D_1). Wear rate decreases with SiC and Gr reinforcement; however, with increase in sliding distance, applied normal load and sliding speed there is increase in wear rate, the same trend of wear parameters was also reported by other authors [27, 37]. The observed statistical results may be attributed to the solid lubricant graphite providing the self-lubricating effect during the dry sliding of AZ91D-SiC-Gr hybrid composite. The addition of graphite content (5 wt%), the wear rate of fabricated hybrid composites was improved over a wide range of applied load, sliding speed and distance. The smearing of graphite in between the sliding counterparts forms a lubricating film thereby reducing the wear rate which has been observed during sliding tests presented in the succeeding

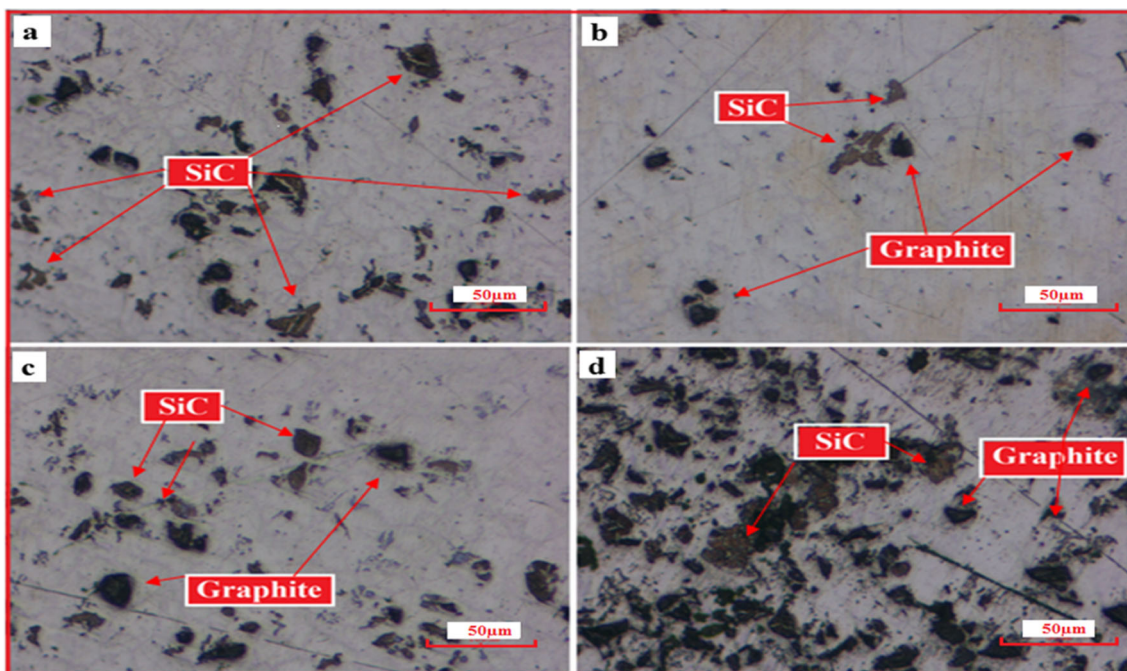
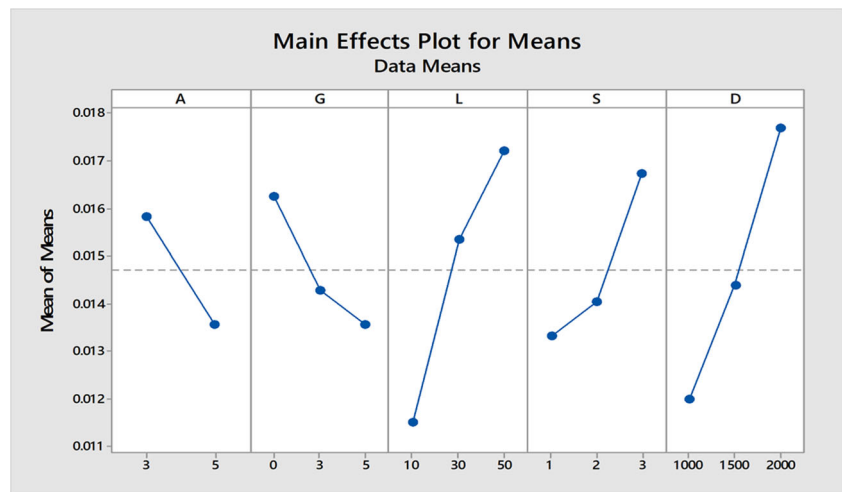


Fig. 4 Micrograph of hybrid magnesium composites **a** AZ91 + 5SiC, **b** AZ91D + 3SiC + 3Gr, **c** AZ91D + 5SiC + 3Gr, and **d** AZ91D + 5SiC + 5Gr

Fig. 5 Main effect plot for data means of control parameters considered on volumetric wear rate as per Table 3



sections of the article. However, mechanical mixed layer (MML) was also formed due to peel out of silicon carbide and graphite at the interface. This MML further reduces the wear rate by decreasing the direct contact between the sliding counterparts. With increase in normal applied load wear mechanism change from mild oxidation to delamination resulting in increased wear rate. Increase of the applied load and sliding distance make more contact between the pin to disc contact surface resulting in the increase in wear loss [42].

3.3 ANOVA

In order to obtain a concrete visualization of the effect of input parameters on the response parameter i.e. volumetric wear

rate, a standard statistical technique ANOVA was performed [43, 44]. The ANOVA table was formulated using Minitab 18 software that determines the influence of individual input parameters, their intersection and percentage contribution of each control factors on the wear rate of fabricated hybrid magnesium composites. From Table 6, it is concluded that a sliding distance(31.85%) have the strongest influence on the volumetric wear rate of AZ91D-SiC-Gr magnesium hybrid composites followed by applied load(30.88%) and sliding speed (12.25), graphite content(7.33%); while SiC content (7.15%) have the least impact. Moreover, the intersections effect of different input variables such as A*G (1.97%), A*L (1.80%) and G*L (0.67%) exhibited negligible effect on wear rate of fabricated hybrid composites.

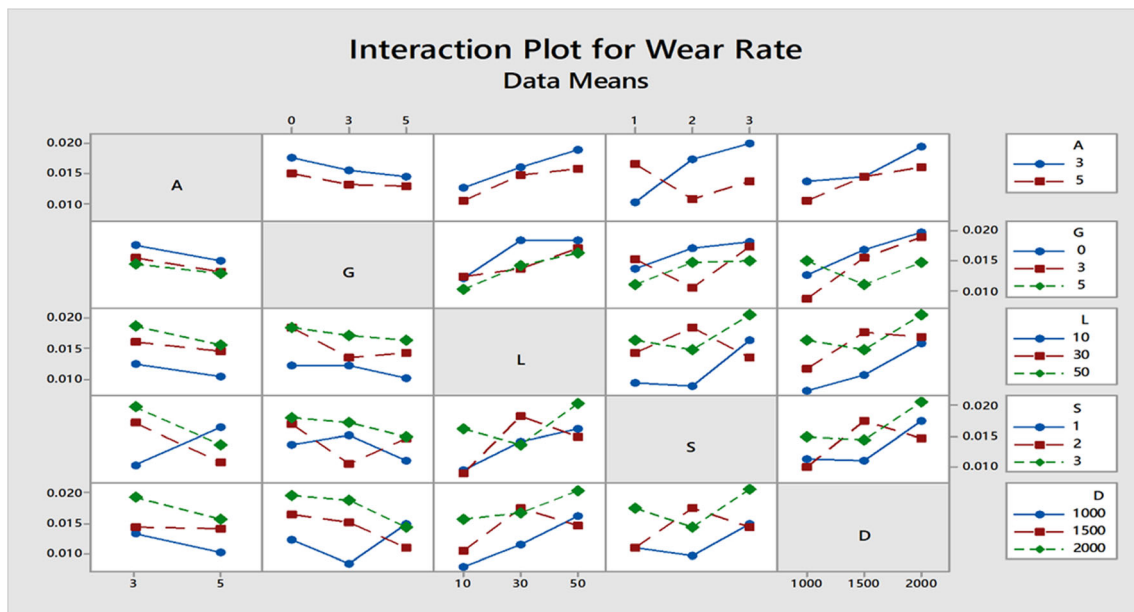


Fig. 6 Interaction plot for various control parameters on wear rate of hybrid composites

Table 6 Analysis of variance of mean value for volumetric wear rate

Source	DF	Seq SS	Contribution	Adj SS	Adj MS	F-Value	P value
A	1	0.000023	7.15%	0.000023	0.000023	37.91	0.025
G	2	0.000023	7.33%	0.000023	0.000012	19.44	0.049
A*G	2	0.00002	6.14%	0.00002	0.00001	16.29	0.058
L	2	0.000102	31.85%	0.000102	0.000051	84.43	0.012
A*L	2	0.000008	2.58%	0.000008	0.000004	6.85	0.127
G*L	2	0.000005	1.44%	0.000005	0.000002	3.81	0.208
S	2	0.000039	12.25%	0.000039	0.00002	32.48	0.03
D	2	0.000099	30.88%	0.000099	0.000049	81.87	0.012
Error	2	0.000001	0.38%	0.000001	0.000001		
Total	17	0.00032	100.00%				

Figure 7a presents the contour plot, wherein the influence of intersection between SiC and graphite content on volumetric wear rate is specified by the curved line. The 3-D response surface plots of wear rate vs. combination of SiC and Graphite content have been generated. From the conducted analysis and contour plots, it was found that volumetric wear rate was minimal at 5 wt.% of SiC and Graphite content each and wear resistance was decreased at low level of both SiC and graphite.

Figure 8a contour graph of volumetric wear rate for applied load and SiC content suggests the existence of effect of intersection between load and SiC percentage. Whereas, Fig. 8b demonstrates response plot of wear rate with various combination of load and SiC. From examining the contour plot and response surface plot it was figured that wear rate was minimal at higher SiC content at 5 wt.% and lower normal applied load of 10 N.

3.3.1 Multiple Linear Regression Models

A multiple linear regression model linked the independent input and output response variable [12, 37, 38]. In the present case, a regression equation generated the linear correlation between the influencing input variables i.e. SiC%(A),

Gr%(G), applied load(L), sliding distance(D) and sliding speed(S) with the wear rate of fabricated hybrid composite. The regression equation generated for the volumetric wear rate of AZ91D-SiC-Gr hybrid composites was elaborated as below:

$$\begin{aligned} \text{Wear Rate} = & 0.00439 - 0.001128 A - 0.000550 G \\ & + 0.000143 L + 0.001717 S \\ & + 0.000006 D \end{aligned} \quad (5)$$

The Eq. (5) specified that the volumetric wear rate decrease with SiC and Graphite reinforcement, while it increase with increase in sliding distance, sliding speed and applied load.

3.3.2 Confirmation Test

A confirmatory test has been accomplished to examine the quality characteristics of the fabricated hybrid magnesium composites by selecting the optimal combination of input parameters. The predicted optimum volumetric wear rate was evaluated by taking into account the influence of each parameter i.e. A_2, G_3, L_1, S_1 and D_1 as given in Fig. 5.

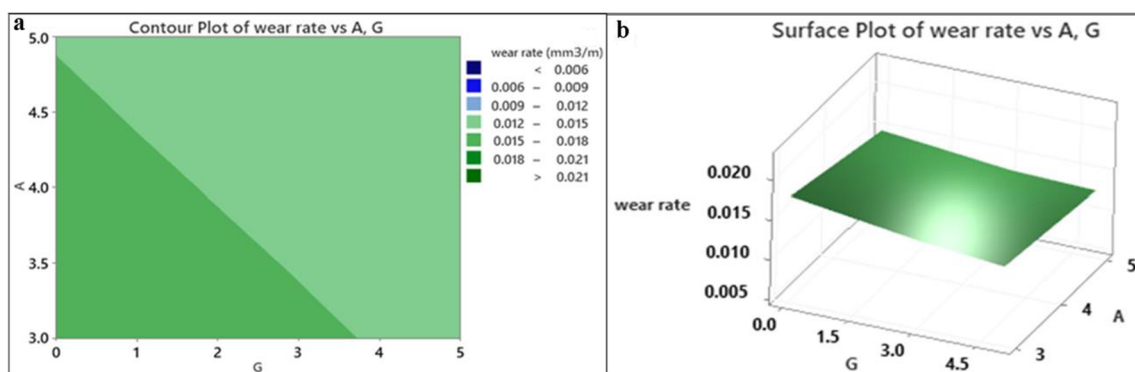


Fig. 7 Contour plot (a) and response plot (b) of wear rate for Graphite content and SiC percentage

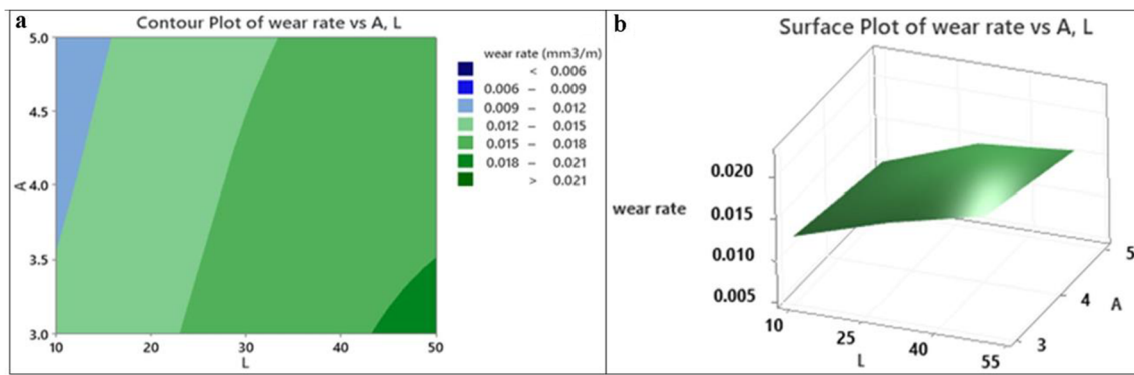


Fig. 8 Contour plot (a) and response plot (b) of wear rate for applied load and SiC percentage

$$Wr = Tw + (A_2 - Tw) + (G_3 - Tw) + (L_1 - Tw) + (S_1 - Tw) + (D_1 - Tw) \tag{6}$$

Where, Wr is volumetric wear rate, Tw is volumetric wear rate - total mean value and A_2, G_3, L_1, S_1 and D_1 are S/N

ratio value for control factors at designated levels. Using Eq. 6, optimal value of volumetric wear rate (Wr) was calculated as $0.0147 \text{ mm}^3/\text{m}$.

The confidence interval for verification of quality characteristics of confirmation test was calculated using Eq. 7 [36, 45, 46].

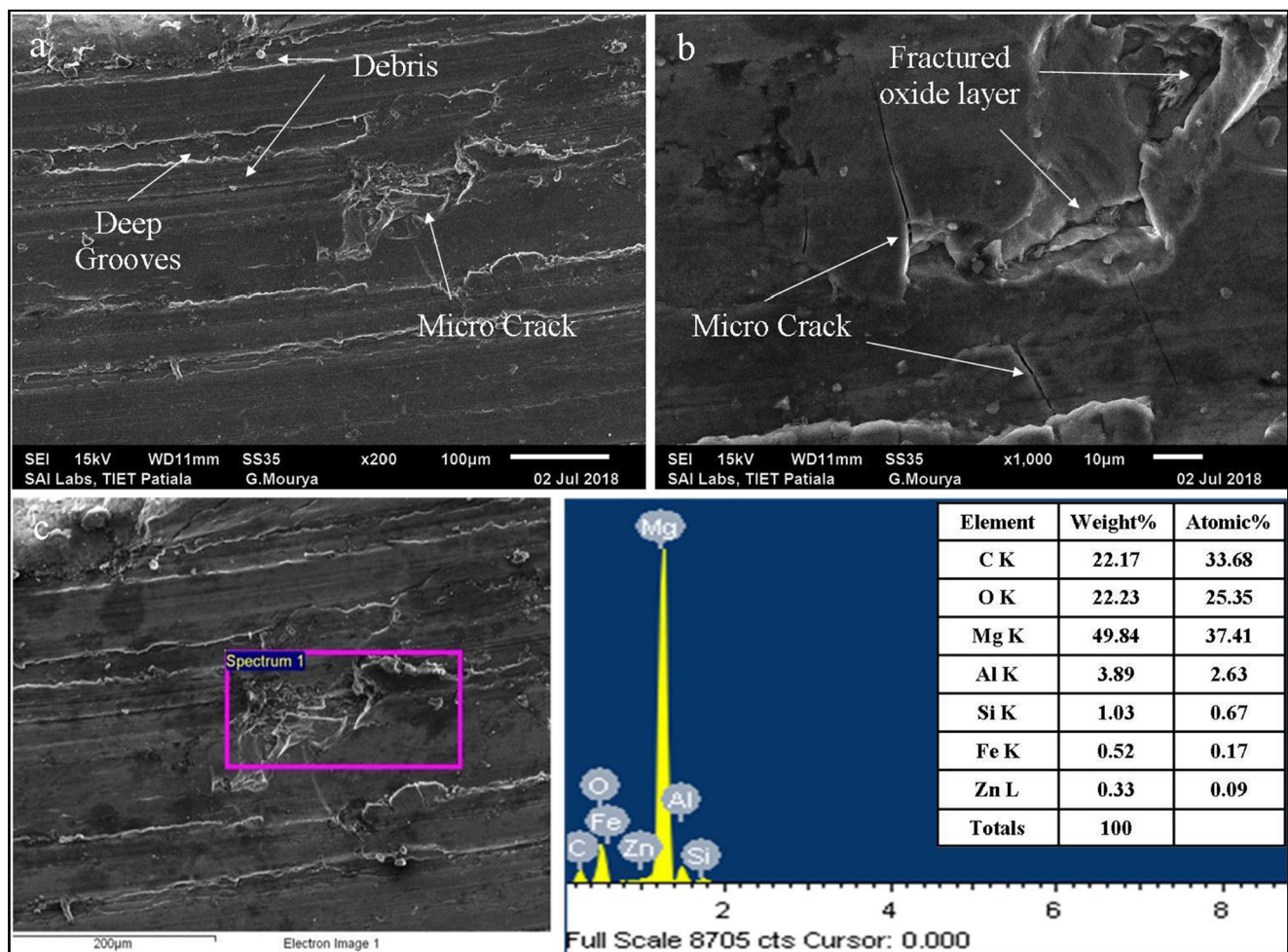


Fig. 9 FESEM image of the worn surface of AZ91D-5 SiC hybrid composite: a at lower magnification, b at higher magnification, c EDS analysis of hybrid composite

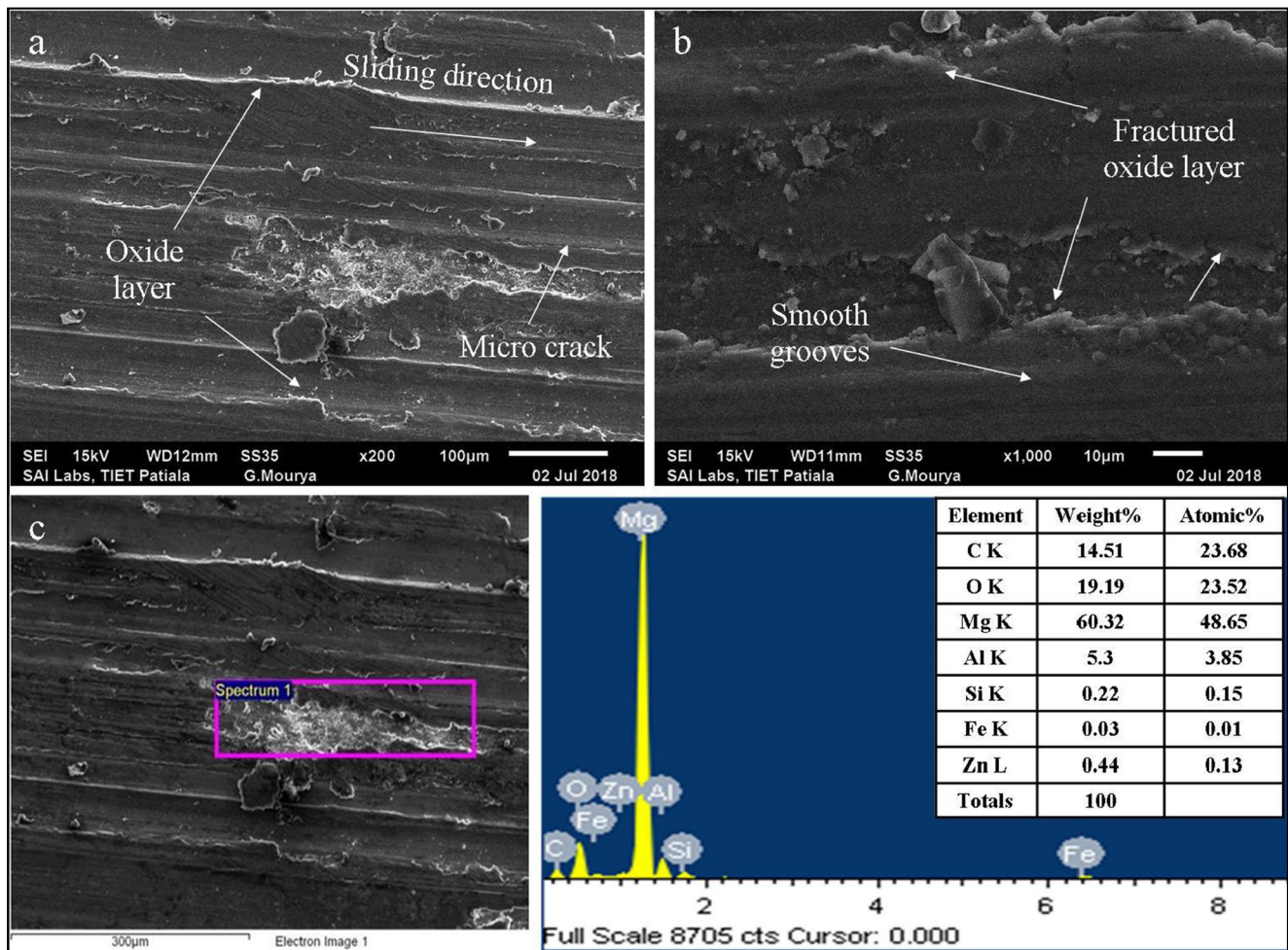


Fig. 10 FESEM image of the worn surface of AZ91D-5 SiC-3Gr hybrid composite: **a** at lower magnification, **b** at higher magnification, **c** EDS analysis of hybrid composite

$$CI = \sqrt{F_{\alpha;1, V_2} \cdot V_{error} \cdot \left(\frac{1}{n_{eff}} + \frac{1}{R} \right)} \quad (7)$$

$F_{\alpha;1, V_2}$ has obtained from the F table at desire level of confidence α and V_2 . V_2 denotes total degree of freedom of variance error. V_{error} denotes error variance, R is number of trial of each experiment, n_{eff} is the number of effective measured results defined in Eq. (8)

$$n_{eff} = \frac{\text{Total experimental runs}}{1 + (\text{total degree of freedom of factors for prediction})} \quad (8)$$

In the present statistical analysis, two repetition of each confirmation test were performed to evaluate the performance of experimental trail for volumetric wear rate under optimal conditions. From the F table, $F_{\alpha;1, V_2}$ for 95% confidence level ($\alpha = 0.05$) was 18.51. Using Eqs. 5 and 6, confidence interval was calculated as ± 0.00519 . The interval in which results of value of wear rate at optimal

setting expected was 0.0051 ± 0.0040 or 0.0011 to 0.0091 with 95 confidence interval. Repetitions of two experiments with optimal settings of A_2, G_3, L_1, D_1 , and S_1 were performed and average value of wear rate in terms of S/N ratio was $0.0034 \text{ mm}^3/\text{m}$, which was within the desired interval.

3.4 Worn Surface Analysis

Surface of worn out specimens of hybrid magnesium composites were investigated using FESEM with an attachment of EDS for understanding of wear mechanism. FESEM of worn out surfaces of AZ91D-5SiC composite and AZ91D-5SiC-3Gr have been shown in Figs. 9a, b and 10a, b respectively. Moreover, Fig. 11 shows the wear surface analysis of AZ91D-5SiC-5Gr hybrid composites at optimal conditions i.e. 1 m/s sliding speed, 500 m sliding distance and 10 N load. For AZ91D-SiC composite, deep and narrow grooves were surrounded with obvious oxidative area and debris due to more material deterioration, as observed in Fig. 9, which

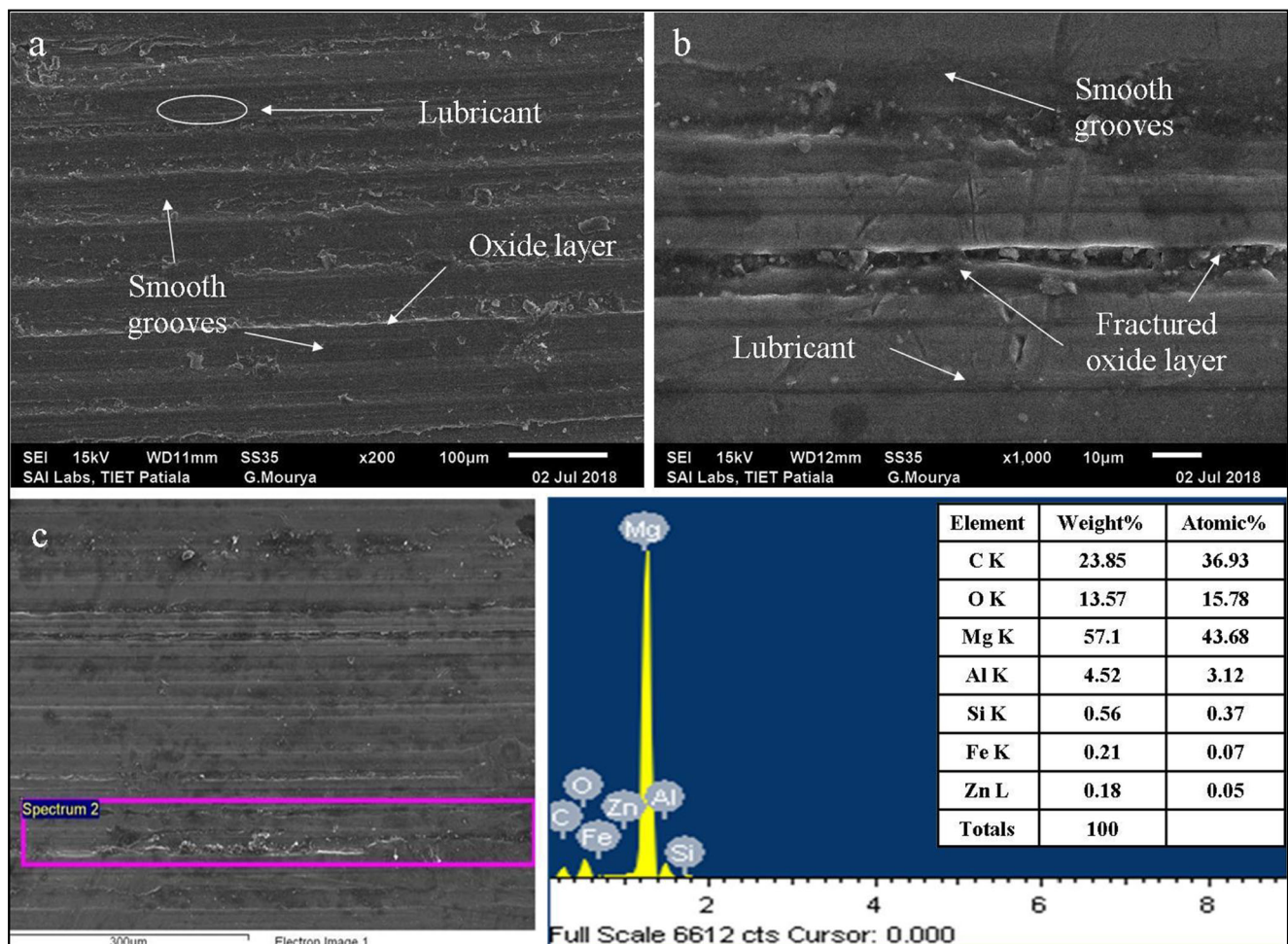


Fig. 11 FESEM image of the worn surface of AZ91D-5 SiC-5Gr hybrid composite: **a** at lower magnification, **b** at higher magnification, **c** EDS analysis of hybrid composite

indicates the presence of abrasive and oxidization wear. From the EDS of the worn surface of AZ91D-5SiC shown in Fig. 9c, it was examined that fabricated magnesium composite indicated higher intensity of peaks of oxygen and formation of oxide layers than the hybrid magnesium composite [42]. Deep grooves were due to the rubbing acting of hard asperities of steel counter plate against the magnesium composite.

It was examined from the Figs. 10 and 11 that these deep grooves were transformed into smooth and shallow for the AZ91D-SiC-Gr hybrid composite reinforced with graphite due to reduced abrasive wear and hence lower plastic deformation. However, fractured oxide layer associated with some micro cracks at higher magnification was also observed. Moreover; for AZ91D-SiC-Gr hybrid composite during dry sliding, SiC reduced the deformation zones by obstructing the plastic flow of base matrix, while a self-lubricating layer of graphite was formed between the sliding counterparts resulting in lower wear rate and improved wear resistance. It was observed that graphite act as polishing agent between the specimen pin and the opposite sliding plate. Also, reinforcement of 5 wt% graphite in AZ91D-5SiC composite results in

formation and removal of MML which enhances the adhesion support between sliding counterparts. The formation of thin MML layer has also been observed by Kumar et al. [41] for Mg-TiC-MoS₂ hybrid magnesium composites and by Prakash et al. [40] for Mg-SiC-Gr hybrid magnesium composites. However, some brittle fracture of magnesium hybrid composite can be seen in Fig. 11 as graphite reinforcement reduced the fracture toughness of fabricated hybrid composite.

The rise in temperature of worn surface due to heat generation during sliding is also an important factor for wear mechanism. The surface with greater heat generation gets oxidized easily and more prone to adhesive wear [10]. In case of AZ91D-SiC-Gr hybrid composite slower temperature rise and few oxidized layer was observed due to self-lubrication effect of graphite resulting in the reduction of adhesion wear. The slower rise in temp is also stated by Prakash et al. [40] for the Mg hybrid composite reinforced with SiC and graphite as compared to pure magnesium. The formation of lubricant film of graphite between the sliding counterparts delays the transition of abrasion and adhesion wear to delamination wear, which results the improved wear resistance [47]. The

delamination wear mechanism alone leads to more wear, but graphite smearing effect and MML formation reduces the overall wear of the hybrid composites. So main dominant wear mechanism observed for AZ91D-SiC-Gr hybrid magnesium composite was delamination.

The EDS spectrum of AZ91D-5SiC-3Gr and AZ91D-5SiC-5Gr hybrid composites was shown in Figs. 10c and 11c respectively. It was found that oxygen peaks are less extensive for AZ91D-5SiC-5Gr hybrid composites and there were lower fractured oxide layers than other fabricated hybrid composites. The EDS spectrums confirm the existence of magnesium, SiC and graphite in hybrid magnesium composites. The results obtained indicated that lubricant layers were the combination of SiC and graphite with iron oxides and other elements.

4 Conclusions

Environment friendly self-lubricating AZ91D-SiC-Gr hybrid composites were successfully fabricated using vacuum assisted bottom pouring stir casting, in pursuit of green tribology, sustainability and energy efficiency. Taguchi's statistical approach was used to analyze sliding wear behavior of fabricated hybrid magnesium composites. The key experimental conclusions obtained from the study are enumerated as follows:

- i. Wear rate of AZ91D-SiC-Gr hybrid magnesium composites was decreased with increase in SiC and graphite particles content. However; wear rate was increased at higher sliding speed, sliding distance and normal load.
- ii. Micro-hardness ($HV_{0.1}$) of fabricated hybrid magnesium composite increased with SiC reinforcement while it decreased with addition of soft graphite.
- iii. The optimal control factors revealed through S/N ratio analysis for minimum wear rate of fabricated hybrid composite was 5 wt% SiC, 5 wt% graphite, 10 N applied load, 1 m/s sliding speed and 500 m sliding distance.
- iv. ANOVA results demonstrated that all five input control factors significantly influenced the wear rate of fabricated hybrid composites. The applied load has the highest influence (31.85%) followed by sliding distance, sliding speed, graphite content and SiC percentage.
- v. The solid lubricant graphite provided the self-lubricating effect in AZ91D-SiC-Gr hybrid composite. The formation of lubricant film of graphite between the sliding counterparts delay the transition of abrasion and adhesion wear to delamination wear resulting the improved wear resistance.
- vi. FE-SEM and EDS analysis of the worn surfaces after wear tests revealed that the dominant wear mechanism of AZ91D-SiC-Gr hybrid composites was delamination; however, AZ91D-SiC composite showed oxidative besides abrasive wear.

References

1. Campbell FC (2012) *Lightweight materials-understanding the basics*. ASM international, Ohio
2. Banerjee S, Poria S, Sutradhar G, Sahoo P (2019) Dry sliding tribological behavior of AZ31-WC nano-composites. *J Magnes Alloy* 7:315–327
3. Li N, Chen Y, Deng B, Yue J, Qu W, Yang H, He Y, Xia W, Li L (2019) Low temperature UV assisted sol-gel preparation of ZrO₂ pore-sealing films on micro-arc oxidized magnesium alloy AZ91D and their electrochemical corrosion behaviors. *J Alloys Compd* 792:1036–1044
4. Yu W, Chen D, Tian L, Zhao H, Wang X (2019) Self-lubricate and anisotropic wear behavior of AZ91D magnesium alloy reinforced with ternary Ti₂AlC MAX phases. *J Mater Sci Technol* 35:275–284
5. Zafari A, Ghasemi H, Mahmudi R (2012) Tribological behavior of AZ91D magnesium alloy at elevated temperatures. *Wear* 292–293: 33–40
6. Dey A, Pandey KM (2015) Magnesium metal matrix composites - a review. *Rev Adv Mater Sci* 42:58–67
7. Girish B, Satish B, Sarapure S, Somashekar D, Basawaraj S (2015) Wear behavior of magnesium alloy AZ91 hybrid composite materials. *Tribol Trans* 58(3):481–489
8. Khatkar SK, Suri N, Kant S, Pankaj (2018) A review on mechanical and tribological properties of graphite reinforced self-lubricating hybrid metal matrix composites. *Rev Adv Mater Sci* 56:1–20
9. Poddar P, Srivastava V, De P, Sahoo K (2007) Processing and mechanical properties of SiC reinforced cast magnesium matrix composites by stir casting process. *Mater Sci Eng A* 460–461: 357–364
10. Aatthisugan I, Rose AR, Jebadurai D (2017) Mechanical and wear behaviour of AZ91D magnesium matrix hybrid composite reinforced with boron carbide and graphite 5:20–35
11. Chourasiya SK, Gautam G, Singh D (2020) Mechanical and tribological behavior of warm rolled Al-6Si-3graphite self lubricating composite synthesized by spray forming process. *Silicon* 12:831–842
12. Ravindran P, Manisekar K, Rathika P, Narayanasamy P (2013) Tribological properties of powder metallurgy - processed aluminium self lubricating hybrid composites with SiC additions. *Mater Des* 45:561–570
13. Ram Prabhu T, Varma V, Vedantam S (2014) Tribological and mechanical behavior of multilayer Cu/SiC + Gr hybrid composites for brake friction material applications. *Wear* 317:201–212
14. Li JL, Xiong D (2008) Tribological properties of nickel-based self-lubricating composite at elevated temperature and counterface material selection. *Wear* 265:533–539
15. Babic M, Slobodan M, Džunic D, Jeremic B, Ilija B (2010) Tribological behavior of composites based on ZA-27 alloy reinforced with graphite particles. *Tribol Lett* 37:401–410
16. Khatkar SK, Verma R, Kant S, Suri NM (2020) In: Pant M, Sharma T, Verma O, Singla R, Sikander A (eds) *Soft computing: theories and applications. Advances in intelligent systems and computing*, vol 1053. Springer, Singapore
17. Feng Y, Wang J, Zhang M, Xu Y (2007) The influence of pressure on the electrical tribology of carbon nanotube-silver-graphite composite. *J Mater Sci* 42:9700–9706

18. Cui G, Bi Q, Niu M, Yang J, Liu W (2013) The tribological properties of bronze-SiC-graphite composites under sea water condition. *Tribol Int* 60:25–35
19. Menezes P, Reeves C, Rohatgi P (2013) In: Menezes PL, Ingole SP, Nosonovsky M, kailas SV, Lovell MR (eds) *Tribology for scientists and engineers: from basics to advanced concepts* 1st edn. Springer Science, New York
20. Moghadam A, Omrani E, Menezes P, Rohatgi P (2015) Mechanical and tribological properties of self-lubricating metal matrix nanocomposites reinforced by carbon nanotubes (CNTs) and graphene: a review. *Compos Part B* 77:402–420
21. Reeves CJ, Menezes PL, Lovell MR (2013) In: Menezes PL, Ingole SP, Nosonovsky M, kailas SV, Lovell MR (eds) *Tribology for scientists and engineers: from basics to advanced concepts* 1st edn. Springer Science, New York
22. Prasad RA, Vamsi KP, Rao RN (2019) Tribological behaviour of Al6061–2SiC-xGr hybrid metal matrix nanocomposites fabricated through ultrasonically assisted stir casting technique. *Silicon* 11: 2853–2871
23. Guo MLT, C-YA T (2000) Tribological behavior of self-lubricating aluminium/SiC/graphite hybrid composites synthesized by the semi-solid powder-densification method. *Compos Sci Technol* 60: 65–74
24. Bodunrin M, Alaneme KK, Chown LH (2015) Aluminium matrix hybrid composites: A review of reinforcement philosophies; mechanical, corrosion and tribological. *Integr Med Res* 4:434–445
25. Mosleh-Shirazi S, Akhlaghi F, Li DY (2016) Effect of graphite content on the wear behavior of Al/2SiC/Gr hybrid nanocomposites respectively in the ambient environment and an acidic solution. *Tribol Int* 103:620–628
26. Xiao JK, Zhang L, Zhou KC, Wang XP (2013) Microscratch behavior of copper-graphite composites. *Tribol Int* 57:38–45
27. Ramesh CS, Noor Ahmed R, Mujeebu M, Abdullah MZ (2009) Development and performance analysis of novel cast copper–SiC–Gr hybrid composites. *Mater Des* 30:1957–1965
28. Mahdavi S, Akhlaghi F (2011) Effect of the graphite content on the tribological behavior of Al/Gr and Al/30SiC/Gr composites processed by in situ powder metallurgy (IPM) method. *Tribol Lett* 44:1–12
29. Krishnaa M, Xavier A (2014) An investigation on the mechanical properties of hybrid metal matrix composites. *Proc Eng* 97:918–924
30. Kaushik N, Rao RN (2016) The effect of wear parameters and heat treatment on two body abrasive wear of Al – SiC – Gr hybrid composites. *Tribol Int* 96:184–190
31. Maamari A, Iqbal K, Nuruzzaman D (2019) Wear and mechanical characterization of Mg–Gr self-lubricating composite fabricated by mechanical alloying. *J Magnes Alloy* 7:283–290
32. Wang C, Deng K, Bai Y (2019) Microstructure, and mechanical and Wear properties of Grp/AZ91 magnesium matrix composites. *Materials* 12:1190–1206
33. Wu Y, Wu K, Deng K, Nie K, Wang X, Zheng M, Hu X (2010) Damping capacities and microstructures of magnesium matrix composites reinforced by graphite particles. *Mater Des* 31:4862–4865
34. Zhu J, Qi J, Guan Q, Ma L, Joyce R (2020) Tribological behaviour of self-lubricating Mg matrix composites reinforced with silicon carbide and tungsten disulfide. *Tribol Int* 146 article no.106253
35. Gowrishankar TP, Manjunatha LH, Sangmesh B (2019) Mechanical and wear behaviour of Al6061 reinforced with graphite and TiC hybrid MMC's. *Mater Res Innov* 24(3):179–185
36. Stojanovic B, Babic M, Velickovic S, Blagojevic J, Velickovic S (2016) Tribological behavior of aluminum hybrid composites studied by application of factorial techniques. *Tribol Trans* 59:522–529
37. Kaushik N, Rao R (2016) Tribology international effect of applied load and grit size on wear coefficients of Al 6082 – SiC – Gr hybrid composites under two body abrasion. *Tribol Int* 103:298–308
38. Senthilkumar M, Saravanan S, Shankar S (2015) Dry sliding wear and friction behavior of aluminum–rice husk ash composite using Taguchi's technique. *J Compos Mater* 49:2241–2250
39. Ekici E, Motorcu A, Kuş A (2016) Evaluation of surface roughness and material removal rate in the wire electrical discharge machining of Al/B4C composites via the Taguchi method. *J Compos Mater* 50:2575–2586
40. Prakash S, Balasundar P, Nagaraja S, Gopal P, Kavimani V (2016) Mechanical and wear behaviour of Mg-SiC-Gr hybrid composites. *J Magnes Alloy* 4(3):197–206
41. Aravindan S, Rao P, Ponappa (2015) Evaluation of physical and mechanical properties of AAZ91D/SiC composites by two step stir casting process. *J Magnes alloy* 3:52–62
42. Selvakumar N, Narayanasamy P (2016) Optimization and effect of weight fraction of MoS2 on the tribological behaviour of Mg-TiC-MoS2. *Tribol Trans* 59:733–747
43. Gopal PM, Prakash S (2019) Wire electric discharge machining of silica rich E-waste CRT and BN reinforced hybrid magnesium MMC. *Silicon* 11:1429–1440
44. Verma R, Suri NM, Kant S (2019) Process optimization of slurry spray technique through multi-attribute utility function. *Arab J Sci Eng* 44(2):919–934
45. Kavimani V, Prakash KS, Thankachan, Nagaraja S, Jeevanantham AK, Jhon JP (2019) WEDM Parameter Optimization for Silicon@r-GO/Magnesium composite using taguchi based GRA coupled PCA. <https://doi.org/10.1007/s12633-019-00205-6>
46. Vijayabhaskar S, Rajmohan T (2019) Experimental investigation and optimization of machining parameters in WEDM of nano-SiC particles reinforced magnesium matrix composites. *Silicon* 11: 1701–1716
47. Gopal P, Prakash K, Nagarajab S, Aravintha N (2017) Effect of weight fraction and particle size of CRT glass on the tribological behaviour of Mg-CRT-BN hybrid composites. *Tribol Int* 116:338–350

Publisher's Note Springer Nature remains neutral with regard to jurisdictional claims in published maps and institutional affiliations.